Dynamic Geometric Equivariant Network for Full-Atom Antibody Design

Weihong Huang[1], **Feng Yang**[1], **Qiang Zhang**[1], **Juan Liu**[2,1*]

[1]School of Computer Science, Wuhan University
[2]School of Artificial Intelligence, Wuhan University
{2023102110011, feng.yang, qiangzhang_, liujuan}@whu.edu.cn

Abstract

Antibody design is critically important in biomedical and therapeutic contexts but remains extremely challenging due to the complexity of antibody sequence–structure relationships and stringent antigen specificity requirements. Traditional computational approaches rely on multi-stage pipelines and often overlook full-atom details (e.g., side-chain conformations) as well as fine-grained geometric features, resulting in limited effectiveness. To overcome these limitations, we propose Dynamic Geometric Equivariant Network (DGENet), an end-to-end full-atom antibody design model that integrates a geometric-kinematic equivariant dynamic optimization module (GK-EDO) with an full-atom E(3)-equivariant message-passing architecture. This framework enables iterative optimization of antibody structures under explicit geometric and kinematic constraints, generating complete antibody structures (including backbone and side chains) and simultaneously jointly optimizing the sequences and 3D structures of the complementarity-determining regions (CDRs). DGENet also introduces a novel virtual anchor docking mechanism that employs an adaptive PNet-Kabsch module to explicitly guide antibody–antigen binding and achieve precise bound conformations. Evaluations on multiple benchmark datasets demonstrate that DGENet exhibits outstanding performance in antibody structure and sequence generation as well as in designing high-affinity antibodies, underscoring its reliability as an advanced antibody design model.

Introduction

Antibodies, as key molecules in biological therapy, are crucial in contemporary medicine. As core effector molecules of the adaptive immune response, antibodies are highly specific immunoglobulins produced by the body. They can precisely recognize and bind specific epitopes on pathogens or abnormal cells, thereby neutralizing them (Taylor et al. 2021; Yoo et al. 2011). Compared to traditional small-molecule drugs, antibody drugs exhibit significant advantages in clinical treatment due to their exceptional target specificity and higher therapeutic index, effectively reducing off-target effects while improving efficacy (Imai and Takaoka 2006; Adolf-Bryfogle et al. 2018). Structurally, a typical antibody molecule consists of two identical heavy chains and two identical light chains, linked by disulfide bonds into a basic Y-shaped configuration. The complementarity-determining region (CDR), located at the tips of the antibody variable regions (Variable Region; VH and VL), directly mediates interactions with antigens, and its sequence and structure determine the antibody's binding specificity and affinity. Therefore, the precise design and optimization of highly specific, high-affinity CDRs is critical for developing effective therapeutic antibody drugs.

Traditional computational methods rely on sampling protein sequences and structures from complex biophysical energy functions (Pantazes and Maranas 2010; Lapidoth et al. 2015; Warszawski et al. 2020). These methods are typically time-consuming and prone to becoming trapped in local optima. In contrast, deep generative models are better equipped to capture the high-dimensional features of amino acids while offering superior computational efficiency and accuracy. Recently, with the rapid advancement of protein design algorithms, various deep generative models have been successfully developed and applied in the field of antibody design. Examples include models designed specifically for 1D sequences (Alley et al. 2019; Shin et al. 2021; Saka et al. 2021; Akbar et al. 2022; He et al. 2024) and those that simultaneously design both sequences and spatial structures (Jin et al. 2021; Jin, Barzilay, and Jaakkola 2022; Luo et al. 2022; Kong, Huang, and Liu 2022, 2023; Zhou et al. 2024; Lin et al. 2024).

However, most of these methods focus primarily on designing protein backbone atoms, and some decouple sequence design from structure design through strategies such as designing sequences first followed by folding, or designing scaffolds first followed by sequence matching (Bennett et al. 2025), making it difficult to accurately model the complex relationship between the two. In contrast, full-atom models can directly generate complete structures including side chains. Since the conformation of protein side chains influences protein function (Foote and Winter 1992), the development of full-atom models is critically important for the field of protein design. In light of this, several full-atom protein design models are currently being developed. Specifically in the field of antibody design, Kong et al. (2023) proposed dyMEAN, an end-to-end full-atom antibody de-

*Corresponding author.

sign model that addresses the issue of error accumulation inherent in traditional multi-stage antibody design workflows. Nevertheless, dyMEAN still has room for improvement in refining the geometric structural features of antibodies.

To address and optimize the aforementioned issues, we propose an antibody molecule full-atom design model named DGENet for end-to-end antibody structure and sequence prediction. DGENet possesses robust capabilities for protein geometric structure analysis. It employs a Geometric-Kinematic Equivariant Dynamic Optimizer (GK-EDO) model to extract refined geometric structural features. GK-EDO meticulously processes not only critical geometric features of the backbone—such as dihedral angles, bond angles, and bond lengths—but also the geometric characteristics of side chains. Subsequently, these finely extracted geometric features are propagated and integrated through an equivariant full-atom message-passing model, ultimately generating the antibody's structure and amino acid sequence. Benefiting from the architecture of these two equivariant feature extraction modules, the entire antibody design process strictly adheres to E(3)-equivariance, thereby mitigating the inherent limitations of traditional methods in modeling 3D spatial geometry and physical symmetries. Additionally, we introduce a virtual anchor docking step, where the predicted antibody structure is aligned with the antigen epitope positions using an adaptively learnable PNet-Kabsch module to obtain precise binding conformations. These innovations enable DGENet to collaboratively generate both the sequence and structure of antibody CDRs while incorporating affinity optimization strategies to further enhance antibody binding performance.

- We propose DGENet, an end-to-end, full-atom antibody design model. It generates antibody sequences and 3D structures conditioned on antigens and optimizes known antibodies to improve affinity.
- We designed a joint architecture with a Geometric-Kinematic Equivariant Dynamic Optimization (GK-EDO) module and an full-atom E(3)-equivariant message-passing module. This extracts key geometric features (dihedral angles, bond angles, lengths) and iteratively refines the antibody structure under geometric/kinematic constraints. Furthermore, adaptively weighted PNet-Kabsch module ensures accurate docking and binding conformations.
- Experimental results indicate that DGENet demonstrates excellent performance in both antibody structure/sequence design and high-affinity antibody generation.

Related Work

Computational Antibody Design

Traditional antibody design models have primarily relied on physics-based force field methods (Lapidoth et al. 2015; Warszawski et al. 2020), which typically employ manually constructed statistical energy functions and sampling algorithms, suffering from computational inefficiency. In recent years, significant progress has been made in deep learning-based antibody design, with structural design approaches mainly divided into graph-based and diffusion-based methods. These approaches have collectively advanced the field of antibody sequence-structure co-design through different mechanisms.

Graph-based methods have garnered widespread attention due to their ability to effectively represent the geometric structure of antibody regions. For instance, Jin et al. successively proposed an iterative autoregressive CDR design framework (Jin et al. 2021) and an epitope-informed hierarchical message-passing network (Jin, Barzilay, and Jaakkola 2022). Kong et al. (2022) introduced MEAN (Kong, Huang, and Liu 2022) and its extension dyMEAN (Kong, Huang, and Liu 2023), both utilizing equivariant graph neural networks, with the latter being an end-to-end antibody design model capable of full-atom generation. These works demonstrate the effectiveness of optimizing antigen-binding capabilities under graph-based structural constraints.

On the other hand, diffusion-based methods simulate a gradual generation process from noise to ordered samples, exhibiting unique advantages in capturing complex biological interactions. DiffAb (Luo et al. 2022) achieved antigen-specific CDR generation by integrating residue type and spatial coordinate information, while AbDiffuser (Martinkus et al. 2023) incorporated domain knowledge and physical constraints to construct full-atom antibody structures. These methods complement each other in handling geometric constraints and structural optimization, collectively driving advancements in antibody design.

Methods

In this section, we will provide a detailed introduction to DGENet. First, we will present an overview of antibody design and some notations related to antibody-antigen complexes. Next, we introduce Geometric-Kinematic Equivariant Dynamic Optimizer (GK-EDO), designed to precisely extract geometric structural features of antibodies while iteratively refining atomic coordinates. Subsequently, we describe an iterative mechanism based on graph equivariant message passing, that propagates these geometric features across the variable regions of antibody chains. Finally, we introduce the Virtual Anchor Docking module, which explicitly guides antibody-antigen binding to obtain accurate binding conformations. The overall workflow of DGENet is illustrated in Figure 2.

Preliminaries

A typical antibody molecule, such as the most common immunoglobulin G (IgG), consists of four polypeptide chains covalently linked by disulfide bonds, forming its characteristic Y-shaped structure (as shown in Figure 1). These four chains include two identical heavy chains and two identical light chains. At the tips of the two arms of the Y-shaped structure lie the antibody's variable regions, which are the core domains enabling its specific recognition function. The variable regions comprise the heavy chain variable region (VH) and the light chain variable region (VL), characterized by their highly variable amino acid sequences.

Within each variable region (VH or VL), the amino

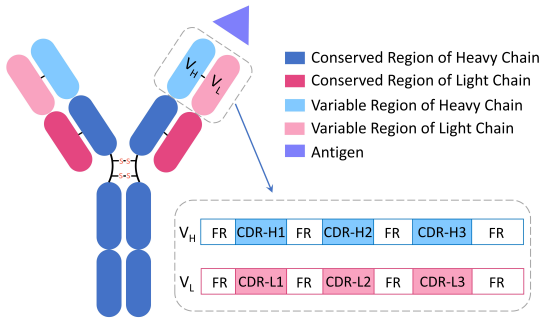

Figure 1: Illustration of antibody-antigen complex structure.

acid sequence is not entirely random but follows a specific pattern: an alternating arrangement of four relatively conserved framework regions (FRs) and three hypervariable complementarity-determining regions (CDRs). Among these, the third complementarity-determining region of the heavy chain variable region (CDR-H3) typically plays a decisive role in the antibody's binding specificity and affinity (Kuroda et al. 2012),due to its most significant sequence and structural diversity. Therefore, precisely predicting the three-dimensional structure of the antibody's variable regions (particularly VH and VL), especially the fine conformation of the framework-supported CDR loops (notably CDR-H3), is paramount for designing novel therapeutic antibodies (Maynard and Georgiou 2000).

Notationd and Task Formulation

This study focuses on antigen-antibody complexes and employs a deep generative modeling approach using a full-atom-resolution graph representation. Specifically, the antibody ariable region and the antigen epitope are modeled as graph structures, denoted as $\mathcal{G}_{AB} = (\mathcal{V}_{AB}, \mathcal{E}^{AB}_{intra})$ and $\mathcal{G}_{AG} = (\mathcal{V}_{AG}, \mathcal{E}^{AG}_{intra})$, respectively, where each node $v_i \in \mathcal{V}_{AB} \cup \mathcal{V}_{AG}$ represents an amino acid residue characterized by the feature representation $\mathcal{V}_i = (a_i, x_i)$, a_i is the amino acid type feature vector, and $x_i \in \mathbb{R}^{M\times 3}$ is the three-dimensional coordinate matrix for all M atoms it contains (M is determined by the amino acid type). Intra-graph edges $\mathcal{E}^{AB}_{intra}$ and $\mathcal{E}^{AG}_{intra}$ are used to capture intra-molecular structural information. Antigen-antibody interactions are modeled by constructing inter-graph edges $\mathcal{E}_{inter}$. The connection rule for these edges is based on the minimum Euclidean distance between all atom pairs of two residues: for a node pair $v_j, v_k \in \mathcal{V}_{AB} \cup \mathcal{V}_{AG}$, an edge ϵ_{jk} exists if and only if

$$\min_{a\in \text{atoms}(v_j), b\in \text{atoms}(v_k)} \|x_a - x_b\|_2 < \tau, \tag{1}$$

where τ is the distance threshold; this method fully integrates the spatial information of side-chain atoms to precisely characterize the molecular interface. Based on this composite graph structure $\mathcal{G} = (\mathcal{V}_{AB} \cup \mathcal{V}_{AG}, \mathcal{E}^{AB}_{intra} \cup \mathcal{E}^{AG}_{intra}, \mathcal{E}_{inter})$, the core task of this study is to develop a deep generative model to predict both the primary structure (i.e, the amino acid type a_j for each node $v_j \in \mathcal{V}_{AB}$) and the three-dimensional structure (i.e, the atomic coordinates x_j for each node $v_j \in \mathcal{V}_{AB}$) of the antibody variable region.

Virtual Anchor Graph and Initialization

In the prediction process of DGENet, we first utilize the antibody template chains provided by Kong et al. (2023) to construct the three-dimensional structure of the antibody as the initial coordinate input for the model. Amino acid positions are encoded using the IMGT numbering scheme (Lefranc et al. 2003) and combined with amino acid type encodings to form the node feature embeddings h_i. Simultaneously, to guide the docking process, we randomly initialize a set of virtual anchors around the antigen epitope based on a standard Gaussian distribution $\mathcal{N}(0, \mathbf{I})$. The number of these virtual anchors equals the number of CDR region nodes in the antibody graph $\mathcal{G}_{AB}$ (i.e., $|\mathcal{V}_{anchor}| = |\mathcal{V}_{cdr}|$), with spatial coordinates denoted as x_i^{anchor}. These anchors share feature embeddings with their corresponding CDR nodes ($h_i^{anchor} = h_i^{cdr}$) and are hypothesized to represent the spatial positions of the true CDR regions after docking. Based on this, we construct the anchor graph $\mathcal{G}_{anchor} = (\mathcal{V}_{anchor}, \mathcal{E}_{anchor})$. Its edge set $\mathcal{E}_{anchor} = (\mathcal{E}^{anchor}_{intra}, \mathcal{E}^{anchor}_{inter})$ comprises two components: the intra-edges $\mathcal{E}^{anchor}_{intra}$ are directly inherited from the internal connections within the CDR region of $\mathcal{G}_{AB}$ (i.e., $\mathcal{E}^{anchor}_{intra} \subseteq \mathcal{E}^{AB}_{intra}$), while the inter-edges $\mathcal{E}^{anchor}_{inter}$ are used to associate $\mathcal{G}_{anchor}$ and $\mathcal{G}_{AG}$, with the distance defined by feature similarity:

$$d(v_i, v_j) = \phi_e(h_i, h_j) + \phi_e(h_j, h_i), i \in \mathcal{V}_{anchor}, j \in \mathcal{V}_{AG}, \tag{2}$$

where ϕ_e is a multi-layer perceptron (MLP).

Geometric-Kinematic Equivariant Dynamic Optimizer

To capture finer-grained geometric features, we developed a dedicated feature extraction model for antibody-related geometric characteristics. Building on the concept of equivariance—inspired by the work of (Huang et al. 2022; Lin et al. 2024)—we propose that atoms experience interaction forces in dynamic force fields (bond lengths, bond angles, dihedral angles). Each atom undergoes displacement under this force, thereby updating its spatial coordinates. For a set of atoms K , we define its corresponding geometric feature type $\mathcal{G}(K)$ based on its atomic count $|K|$:

$$\mathcal{G}(K) = \begin{cases} \text{bond length}, & K = \{i, j\},\ |K| = 2 \\ \text{bond angle}, & K = \{i, j, k\},\ |K| = 3 \\ \text{dihedral angle}, & K = \{i, j, k, l\},\ |K| = 4 \end{cases} \tag{3}$$

We then define the general formula for the motion of atoms under force as:

$$f_{K,i} = \sum_K \varphi_K(x_i, x_r, h_i, h_r, e_{ri}), \tag{4}$$

$$v_i = \mathcal{T}\left(v_i^0, f_{K,i}, x_r\right), \tag{5}$$

$$x_i = x_i^0 + v_i, \tag{6}$$

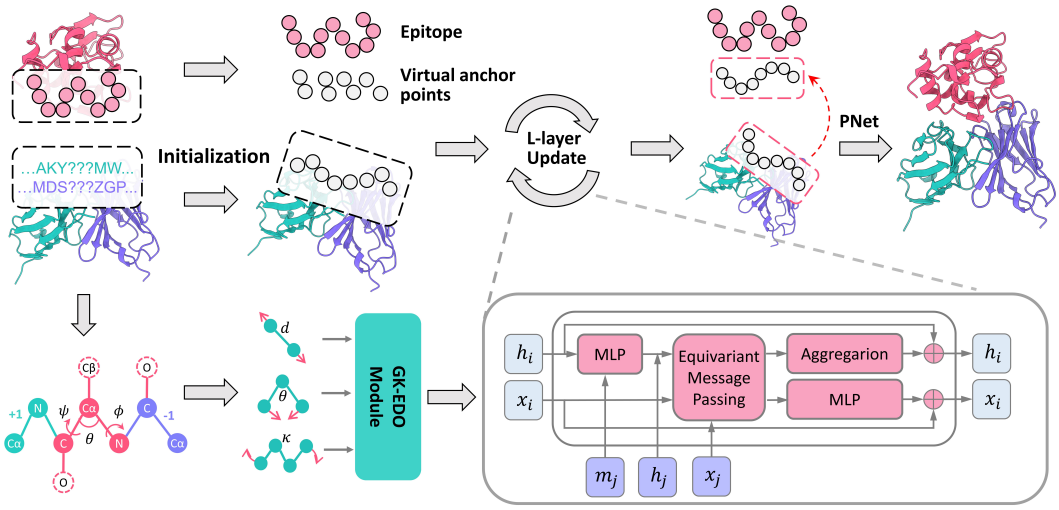

Figure 2: Overview of DGENet. The given antigen epitope and antibody structures are first converted into graph representations for structural initialization, and virtual docking sites are generated around the epitope. Meanwhile, the geometric information of the antibody structure—such as bond lengths, bond angles, and dihedral angles—is fed into the GK-EDO model for refined feature extraction. Subsequently, through L-layers of iterative processing by an equivariant graph neural network, the node embeddings across all graphs are updated. Finally, the designed antibody structure is spatially aligned to the correct position via a virtual site docking module.

where $\mathcal{T}$ is an update function related to the geometric type, $f_{K,i}$ represents the interaction force in this geometric field learned through the function φ_K, $r \in K$ is the fixed reference node, and v_i indicates the velocity of atomic motion.

Specifically, when the geometric context is the bond length:

$$v_i^0 = -\frac{x_j - x_i}{\| x_j - x_i \|_2}, \tag{7}$$

$$\mathcal{T}(v_i^0, f_{K,i}, x_r) = \alpha \cdot f_{K,i} \cdot v_i^0, \tag{8}$$

where α is a step size hyperparameter.

When the geometric context is the bond angle, fixed node $r = j$:

$$v_i^0 = -\frac{(x_i - x_j) \times (x_k - x_j)}{\|(x_i - x_j) \times (x_k - x_j)\|_2}, \tag{9}$$

$$\mathcal{T}(v_i^0, f_{K,i}, x_r) = R(\beta \cdot f_{K,i}, v_i^0) \cdot (x_i - x_j) + x_j - x_i, \tag{10}$$

where $f_{K,i}$ is encoded using the bond angle θ_{ijk} and encoded $[\sin(\theta_{ijk}), \cos(\theta_{ijk})]$.

Similarly, when the geometric context is the dihedral angle, fixed node $r_1 = j, r_2 = k$:

$$v_i^0 = -\frac{(x_j - x_k)}{||(x_j - x_k)||_2}, \tag{11}$$

$$\mathcal{T}(v_i^0, f_{K,i}, x_r) = R(\beta \cdot f_{K,i}, v_i^0) \cdot (x_i - x_j) + x_j - x_i. \tag{12}$$

For dihedral angle, we employ the encoding scheme $[\sin|\kappa_{ijkl}|, \cos|\kappa_{ijkl}|]$, where the absolute value of θ is taken to avoid parity issues. Since dihedral angles exhibit periodicity (where 0° and 360° are equivalent), the absolute value treatment preserves rotational symmetry.

Full-Atom Equivariant Message Passing

Recently, equivariant graph neural networks (EGNNs) have shown remarkable success in the field of protein design (Huang et al. 2022; Han et al. 2025). These models effectively address a key limitation of traditional graph neural networks (GNNs) in coordinate prediction: their outputs fail to guarantee equivariance under input rotations/translations, leading to inconsistent predictions for identical protein structures across different coordinate systems. Similar to (Kong, Huang, and Liu 2022), we adopt EGNN (Satorras, Hoogeboom, and Welling 2021) as the foundational model for our message-passing framework. We perform full-atom equivariant message passing across all graphs, thus updating the amino acid sequence features and 3D coordinates of $\mathcal{V}_{AB}$ and $\mathcal{V}_{anchor}$. We represent the coordinates of each residue using all types of atoms jointly, i.e. $x_i \in \mathbb{R}^{M\times 3}$, where M denotes the number of atom types for that residue. This extends the residue coordinates from a single input vector to multichannel coordinates. Subsequently, we update the information for each node in the following way:

$$m_{ij} = \phi_m\left(h_i^{(l)}, h_j^{(l)}, d_{ij}^{(l)}\right), \tag{13}$$

$$\Delta x_{ij} = \left(x_i^{(l)} - \frac{1}{c_j}\sum_{k=1}^{c_j} x_j^{(l)}(:,k)\right)\phi_x(m_{ij}), \tag{14}$$

$$x_i^{(l+1)} = x_i^{(l)} + \frac{1}{|\mathcal{N}(i)|}\sum_{j\in\mathcal{N}(i)} \Delta x_{ij}, \tag{15}$$

$$h_i^{(l+1)} = \phi_h\left(h_i^{(l)}, \sum_{j\in\mathcal{N}(i)} m_{ij}\right), \tag{16}$$

where $d_{ij}^{(l)} = \min_{1\le p\le c_i, 1\le q\le c_j} \|x_i^{(l)}(:,p) - x_j^{(l)}(:,q)\|_2$ is the minimum inter-atom distance. ϕ_m is an MLP generating invariant messages. The term $\frac{1}{c_j}\sum_k x_j^{(l)}(:,k)$ computes the centroid of residue j, $\mathcal{N}(i)$ represents a neighbor of node i.

Finally, we pass the obtained $h_i^{(l+1)}$ through a softmax function to predict the final amino acid types.

$$s_i^* = Softmax\left(\phi_s(h_i^{(l+1)})\right), \tag{17}$$

where ϕ_s is an MLP, and s_i^* represents the probability distribution over the types for the i-th amino acid residue.

Virtual Anchor Docking

After performing message passing on graphs $\mathcal{G}_{AB}$ and $\mathcal{G}_{anchor}$, we obtained the updated nodes $x_{anchor,i}^{(l+1)}(i \in V_{anchor})$ and $x_{cdr,i}^{(l+1)}(i \in \mathcal{V}_{cdr} \subseteq \mathcal{V}_{AB})$, we achieve docking by aligning them. This operation positions the predicted antibody chain correctly via rigid transformation. To accomplish this, we improve upon the Kabsch algorithm (Kabsch 1976) and propose the PNet-Kabsch module.

During the alignment process, we primarily utilize the four backbone atoms of amino acids, $S = \{N, C_\alpha, C, O\}$. The difference between PNet-Kabsch and Kabsch lies in the calculation of the centroid: we assign different weights to atoms of different types. That is, for any amino acid coordinate a_i, we have:

$$a_i^{centroid} = \frac{1}{\sum_{k=1}^4 w_k}\sum_{k=1}^4 w_k a_k, \tag{18}$$

where the weight vector $w_k \in \mathbb{R}^{4\times 1}$ is adaptively learned through a neural network based on the PointNet (Qi et al. 2017) architecture for point cloud feature extraction. The network's processing is defined as:

$$w_i = \delta\left(fc\left(\max_{s\in S} h_\theta(x_{i,s}^{anchor}, x_{i,s}^{cdr})\right)\right), \tag{19}$$

where δ denotes the softmax activation function, h_θ is the MLP from PointNet, and fc is a fully connected layer. Finally, we align the predicted antibody structure with virtual docking anchors via PNet-Kabsch to obtain the final predicted antibody-antigen complex:

$$Q, t = \mathrm{PK}(\{x_{anchor,i}^{(l+1)} | i \in \mathcal{V}_{anchor}\}, \{x_{cdr,i}^{(l+1)} | i \in \mathcal{V}_{AB}\}), \tag{20}$$

$$x_i^* = Q x_i^{(T)} + t, \quad \forall i \in \mathcal{V}_{AB}, \tag{21}$$

where (Q, t) denotes a rigid transformation (rotation matrix $Q \in SO(3)$, translation vector $t \in \mathbb{R}^3$), PK denotes PNet-Kabsch modoule and x_i^* represents the final predicted antibody 3D coordinates.

Loss Function

We train DGENet using three distinct loss functions: antibody structure loss, virtual anchor docking loss and amino acid sequence loss.

Antibody Structure Loss We classify the antibody structure loss into coordinate loss $\mathcal{L}_{\text{coord}}$ and geometric loss $\mathcal{L}_{\text{geo}}$. For structural optimization, we first use huber loss (Huber 1992) to compute the coordinate loss between predicted and ground-truth 3D coordinates:

$$\mathcal{L}_{\text{coord}} = \frac{1}{|\mathcal{V}_{AB}|}\sum_{i\in\mathcal{V}_{AB}} \ell_{\text{Huber}}(x_i^*, x_i^{True}), \tag{22}$$

where x_i^{True} denotes the ground-truth coordinates. Additionally, we partition the geometric loss $\mathcal{L}_{\text{geo}}$ into three components based on different geometric contexts (bl: bond lengths, ba: bond angles, da: dihedral angles). For the side chains, we first use an MLP to predict the types of amino acids, based on which the relevant geometric information is derived.

$$\mathcal{L}_{bl} = \sum_{(i,j)\in\mathcal{B}} (d_{i,j}^{Pred} - d_{i,j}^{Ture})^2, \tag{23}$$

$$\mathcal{L}_{ba} = \sum_{(i,j,k)\in\mathcal{A}} (\theta_{i,j,k}^{Pred} - \theta_{i,j,k}^{True})^2, \tag{24}$$

$$\mathcal{L}_{da} = \sum_{(i,j,k,l)\in\mathcal{D}} (\kappa_{i,j,k,l}^{Pred} - \kappa_{i,j,k,l}^{Ture})^2, \tag{25}$$

where $\mathcal{B}, \mathcal{A}$, and $\mathcal{D}$ represent sets of bond lengths, bond angles, and dihedral angles, respectively.

Virtual Anchor Docking Loss The virtual anchor docking loss consists of two parts: distance $\mathcal{L}_{\text{dist}}$ and anchor structure loss $\mathcal{L}_{\text{anchor}}$.

$$\mathcal{L}_{\text{dist}} = \frac{1}{|\mathcal{V}_{AG}||\mathcal{V}_{anchor}|}\sum_{(i,j)\in\mathcal{E}_{inter}^{anchor}} \ell_{\text{Huber}}(d_{i,j}^{Pred}, d_{i,j}^{True}), \tag{26}$$

$$\mathcal{L}_{\text{anchor}} = \frac{1}{|\mathcal{V}_{anchor}|}\sum_{i\in\mathcal{V}_{anchor}} \ell_{\text{Huber}}(x_i^{anchor}, x_i^{True}), \tag{27}$$

where the distance d_i^{Pred} is calculated by Eq. 2, x_i^{anchor} is the spatial coordinate of the predicted virtual anchor docking site.

Amino Acid Sequence Loss Amino acid sequence loss are trained via cross-entropy ℓ_{ce}:

$$\mathcal{L}_{\text{seq}} = \frac{1}{|\mathcal{V}_{AB}|}\sum_{i\in\mathcal{V}_{AB}} \ell_{\text{ce}}(s_i^*, s_i^{True}). \tag{28}$$

Results

Evaluation Metrics We use the following metrics for quantitative assessment: 1.AAR: Overlap ratio between generated and reference sequences. 2.lDDT (Mariani et al. 2013): Local distance difference test comparing atomic distance matrices. 3.TMscore (Zhang and Skolnick 2004): Global $C\alpha$ similarity between structures. 4.RMSD: Root Mean Square Deviation. 5.DockQ (Basu and Wallner 2016): Comprehensive antibody-epitope docking quality score. Note: RMSD and DockQ are sensitive to relative antibody-epitope positions.

Model	AAR(↑)	lDDT(↑)	TMscore(↑)	RMSD(↓)	DockQ(↑)
RosettaAb*	32.31%	0.8272	0.9717	17.70	0.137
DiffAb*	35.31%	0.8281	0.9695	23.24	0.158
MEAN*	37.38%	0.8252	0.9688	17.30	0.162
GeoAB*	40.02%	0.8367	0.9695	15.43	0.187
HERN	32.65%	—	—	9.15	0.294
dyMEAN	41.84%	0.8392	0.9718	8.10	0.407
DGENet	**42.67%**	**0.8551**	**0.9747**	**7.19**	**0.431**

Table 1: Results of CDR-H3 design on RAbD. Methods marked with a superscript * follow the pipeline: IgFold→ HDOCK→ CDR design model → Rosetta.

CDR-H3 Sequence Generation and Structural Design

We first evaluated the performance of the DGENet model in the co-design task of sequence and structure for the CDR-H3. Given the decisive role of CDR-H3 in binding specificity and affinity, this evaluation is particularly critical. All models were trained on the SAbDab dataset (Dunbar et al. 2014) and evaluated on the RAbD benchmark set (Adolf-Bryfogle et al. 2018), which comprises 60 distinct antibody-antigen complexes. Following the approach of Jin et al. (2022) complexes were renumbered using the IMGT scheme (Lefranc et al. 2003). The SAbDab dataset was partitioned into training and validation sets at a 9:1 ratio, with the split based on CDR sequence clustering performed by MMseqs2 (Steinegger and Söding 2017) to ensure sequence divergence across training, validation, and test sets. For non-end-to-end backbone structure generation models (e.g., DiffAb, MEAN, GeoAB), we encapsulated them using a pipeline incorporating IgFold (Ruffolo et al. 2023)→ HDOCK (Yan et al. 2020)→ CDR design model → Rosetta (Alford et al. 2017). Furthermore, since HERN (Jin, Barzilay, and Jaakkola 2022) generates only the paratope structure without considering the framework regions, we did not compute TM-score or lDDT for it.

As shown in Table 1, our method demonstrates superior performance across all evaluation metrics, significantly outperforming the second-ranked method, dyMEAN, in all five metrics. This indicates that DGENet offers substantial advantages in achieving fine-grained geometric modeling. Additionally, we visually compared the antibody structures designed by DGENet and dyMEAN (Figure 3). The results demonstrate that structures designed by DGENet exhibit closer resemblance to the real antibody structure overall, with particularly superior performance in the CDR-H3 region. In contrast, dyMEAN designs exhibited minor chain breaks, representing unrealistic structural features. These results indicate that DGENet possesses advantages in the fine-grained modeling of antibody geometry.

Ablation Study

We further conducted ablation experiments on the CDR-H3 generation task to evaluate the effectiveness of each component in DGENet, with the results presented in Table 2. First, we evaluated the impact of full-atom modeling (including

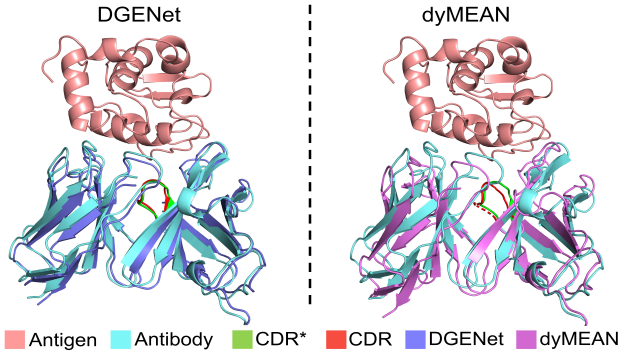

Figure 3: Complexes (pdb: 1ic7) generated by GENet and dyMEAN. CDR* represents the CDR structure of the ground truth, and CDR is the predicted CDR structure.

Model	AAR↑	lDDT↑	TMscore↑	RMSD↓	DockQ↑
Full atom	40.58%	0.7962	0.9689	11.23	0.353
GK-EDO	41.95%	0.8442	0.9732	7.96	0.399
PNet	42.26%	0.8549	0.9747	7.65	0.413
Single-L	40.25%	0.8342	0.9721	8.35	0.398
DGENet	**42.67%**	**0.8551**	**0.9747**	**7.19**	**0.431**

Table 2: Model Performance Comparison

all atoms of amino acid backbones and side chains). The results showed that when the model considered only backbone atoms, DGENet's performance significantly declined, highlighting the importance of full-atom modeling. Second, removing the geometric refinement module (GK-EDO) resulted in a decline across all evaluation metrics, confirming that GK-EDO's refined modeling of geometric structures is crucial for DGENet to achieve precise antibody design. Additionally, we examined the PNet-Kabsch (PNet) module with adaptive weighting capability. Analysis revealed that the adaptive weighting mechanism enhances antibody docking performance, particularly demonstrating a clear improvement in DockQ scores. Finally, it was verified whether single-layer (Single-L) message passing could work, and the

Model	lDDT↑	TMscore↑	RMSD↓	DockQ↑
IgFold→HDOCK	0.8439	0.9701	16.32	0.202
IgFold→HERN	0.8441	0.9702	9.63	0.429
GT→HERN	1.0	1.0	9.65	0.432
dyMEAN	0.8673	0.9731	9.05	0.452
DGENet	**0.8735**	**0.9735**	**7.98**	**0.463**

Table 3: Results of Full Antibody Structure Design

results indicated that it would lead to a performance drop.

Full Antibody Structure Design

In addition to the CDR region design, we evaluated the performance of the DGENet model on the full antibody structure prediction task, which requires predicting the 3D antibody structure from a given antigen structure and the antibody's complete amino acid sequence. All models were trained on the SAbDab dataset using a 9:1 training-to-validation split. To mitigate potential test data leakage risks when comparing against the IgFold model, performance was assessed on the independent test set employed in the IgFold study, comprising 51 antigen-antibody complexes. Given this experiment's focus on full antibody structure prediction rather than solely the CDR regions, we selected HERN and dyMEAN as benchmark models. For HERN, following Kong et al.'s (2023) methodology, we performed two comparative analyses: (1) Using IgFold-predicted structures as input, processed by HERN, and subsequently refined using Rosetta (IgFold → HERN → Rosetta pipeline). (2) Directly optimizing experimentally determined ground-truth structures with HERN (Ground Truth → HERN). As shown in Table 3, the DGENet model demonstrated superior performance in this task: it significantly outperformed dyMEAN in both structural accuracy and docking scores. Remarkably, DGENet's docking score even surpassed the result of HERN optimized using the experimental ground truth structures by approximately 3.1%.

Affinity Optimization

Optimizing the CDR-H3 region of antibodies is a highly effective approach to enhance antibody-antigen affinity. In this experiment, we employed DGENet to optimize the amino acid sequence and structure of the CDR-H3 region, aiming to design stable, high-affinity binding conformations. Following the model training strategy outlined in CDR-H3 design, we similarly divided the SAbDab dataset into training and validation sets in a 9:1 ratio. Antibodies from the SKEMPI V2.0 dataset (Jankauskaitė et al. 2019) were used as the test set. To ensure a fair comparison, we predicted the affinity change ($\Delta\Delta G$) of the optimized antibodies based on a widely used affinity prediction method (Shan et al. 2022). Specifically, we adopted the same approach as dyMEAN, training and fitting a $\Delta\Delta G$ predictor using a multilayer perceptron (MLP), while optimizing the initial conformations of all residues through gradient-based search to pursue higher-affinity complexes. For each antibody in the test set, we generated 50 candidate antibodies, retaining the one with the optimal $\Delta\Delta G$. We then recorded the affinity change ($\Delta\Delta G$) and the number of optimized residues (ΔL) for each protein. Our goal was to achieve the lowest $\Delta\Delta G$ while minimizing ΔL (Ren et al. 2022). We compared DGENet with dyMEAN, MEAN, and DiffAb. The results (Table 4) demonstrate that DGENet, dyMEAN, and MEAN all exhibit superior performance compared to DiffAb. Notably, DGENet achieves a more significant affinity improvement than mean and dyMEAN by modifying the fewest residues, highlighting its potential for designing high-affinity antibodies. Furthermore, we visualized the optimization results using PDB id 1xgr as an example (Figure 4).

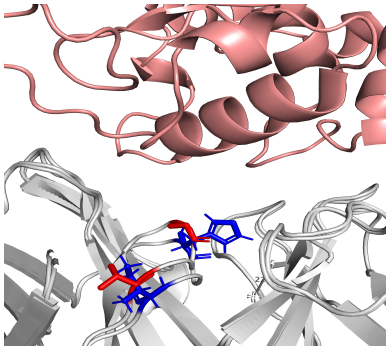

Figure 4: Two key residues in the wild-type antibody (pdb: 1xgr, $\Delta\Delta G$ = -10.61) underwent computational optimization through DGENet to enhance binding affinity. The altered residues are highlighted in blue.

Model	$\Delta\Delta G\downarrow$	$\Delta L\downarrow$
Diffab	-2.17	7.06
MEAN	-6.48	8.96
dyMEAN	-6.75	6.47
DGENet	**-7.41**	**4.33**

Table 4: Results of Affinity Optimization

Conclusion

We introduces DGENet, an end-to-end full-atom antibody design framework based on a Dynamic Geometric Equivariant Network. DGENet incorporates a Geometric-Kinematic Equivariant Dynamic Optimization (GK-EDO) module and an full-atom E(3)-equivariant message-passing architecture. It iteratively optimizes antibody structures under explicit geometric and kinematic constraints, enabling precise geometric feature refinement. Experimental results demonstrate that DGENet outperforms existing methods, highlighting its robust and high-fidelity antibody design capability. This framework provides an effective tool for advancing therapeutic antibody development. Future work will extend DGENet to incorporate explicit physicochemical constraints—such as van der waals forces and steric hindrance—for precise immune complex modeling.

Acknowledgments

This work is supported by the National Key R&D Program of China (No.2019YFA0904303).

References

Adolf-Bryfogle, J.; Kalyuzhniy, O.; Kubitz, M.; Weitzner, B. D.; Hu, X.; Adachi, Y.; Schief, W. R.; and Dunbrack Jr, R. L. 2018. RosettaAntibodyDesign (RAbD): A general framework for computational antibody design. *PLoS computational biology*, 14(4): e1006112.

Akbar, R.; Robert, P. A.; Weber, C. R.; Widrich, M.; Frank, R.; Pavlović, M.; Scheffer, L.; Chernigovskaya, M.; Snapkov, I.; Slabodkin, A.; et al. 2022. In silico proof of principle of machine learning-based antibody design at unconstrained scale. In *MAbs*, volume 14, 2031482. Taylor & Francis.

Alford, R. F.; Leaver-Fay, A.; Jeliazkov, J. R.; O'Meara, M. J.; DiMaio, F. P.; Park, H.; Shapovalov, M. V.; Renfrew, P. D.; Mulligan, V. K.; Kappel, K.; et al. 2017. The Rosetta all-atom energy function for macromolecular modeling and design. *Journal of chemical theory and computation*, 13(6): 3031–3048.

Alley, E. C.; Khimulya, G.; Biswas, S.; AlQuraishi, M.; and Church, G. M. 2019. Unified rational protein engineering with sequence-based deep representation learning. *Nature methods*, 16(12): 1315–1322.

Basu, S.; and Wallner, B. 2016. DockQ: a quality measure for protein-protein docking models. *PloS one*, 11(8): e0161879.

Bennett, N. R.; Watson, J. L.; Ragotte, R. J.; Borst, A. J.; See, D. L.; Weidle, C.; Biswas, R.; Yu, Y.; Shrock, E. L.; Ault, R.; et al. 2025. Atomically accurate de novo design of antibodies with RFdiffusion. *Nature*, 1–11.

Dunbar, J.; Krawczyk, K.; Leem, J.; Baker, T.; Fuchs, A.; Georges, G.; Shi, J.; and Deane, C. M. 2014. SAbDab: the structural antibody database. *Nucleic acids research*, 42(D1): D1140–D1146.

Foote, J.; and Winter, G. 1992. Antibody framework residues affecting the conformation of the hypervariable loops. *Journal of molecular biology*, 224(2): 487–499.

Han, R.; Huang, W.; Luo, L.; Han, X.; Shen, J.; Zhang, Z.; Zhou, J.; and Chen, T. 2025. HeMeNet: Heterogeneous Multichannel Equivariant Network for Protein Multi-task Learning. In *Proceedings of the AAAI Conference on Artificial Intelligence*, volume 39, 237–245.

He, H.; He, B.; Guan, L.; Zhao, Y.; Jiang, F.; Chen, G.; Zhu, Q.; Chen, C. Y.-C.; Li, T.; and Yao, J. 2024. De novo generation of SARS-CoV-2 antibody CDRH3 with a pre-trained generative large language model. *Nature Communications*, 15(1): 6867.

Huang, W.; Han, J.; Rong, Y.; Xu, T.; Sun, F.; and Huang, J. 2022. Equivariant graph mechanics networks with constraints. *arXiv preprint arXiv:2203.06442*.

Huber, P. J. 1992. Robust estimation of a location parameter. In *Breakthroughs in statistics: Methodology and distribution*, 492–518. Springer.

Imai, K.; and Takaoka, A. 2006. Comparing antibody and small-molecule therapies for cancer. *Nature Reviews Cancer*, 6(9): 714–727.

Jankauskaitė, J.; Jiménez-García, B.; Dapkūnas, J.; Fernández-Recio, J.; and Moal, I. H. 2019. SKEMPI 2.0: an updated benchmark of changes in protein–protein binding energy, kinetics and thermodynamics upon mutation. *Bioinformatics*, 35(3): 462–469.

Jin, W.; Barzilay, R.; and Jaakkola, T. 2022. Antibody-antigen docking and design via hierarchical structure refinement. In *International Conference on Machine Learning*, 10217–10227. PMLR.

Jin, W.; Wohlwend, J.; Barzilay, R.; and Jaakkola, T. 2021. Iterative refinement graph neural network for antibody sequence-structure co-design. *arXiv preprint arXiv:2110.04624*.

Kabsch, W. 1976. A solution for the best rotation to relate two sets of vectors. *Foundations of Crystallography*, 32(5): 922–923.

Kong, X.; Huang, W.; and Liu, Y. 2022. Conditional antibody design as 3d equivariant graph translation. *arXiv preprint arXiv:2208.06073*.

Kong, X.; Huang, W.; and Liu, Y. 2023. End-to-end full-atom antibody design. *arXiv preprint arXiv:2302.00203*.

Kuroda, D.; Shirai, H.; Jacobson, M. P.; and Nakamura, H. 2012. Computer-aided antibody design. *Protein engineering, design & selection*, 25(10): 507–522.

Lapidoth, G. D.; Baran, D.; Pszolla, G. M.; Norn, C.; Alon, A.; Tyka, M. D.; and Fleishman, S. J. 2015. Abdesign: A n algorithm for combinatorial backbone design guided by natural conformations and sequences. *Proteins: Structure, Function, and Bioinformatics*, 83(8): 1385–1406.

Lefranc, M.-P.; Pommié, C.; Ruiz, M.; Giudicelli, V.; Foulquier, E.; Truong, L.; Thouvenin-Contet, V.; and Lefranc, G. 2003. IMGT unique numbering for immunoglobulin and T cell receptor variable domains and Ig superfamily V-like domains. *Developmental & Comparative Immunology*, 27(1): 55–77.

Lin, H.; Wu, L.; Huang, Y.; Liu, Y.; Zhang, O.; Zhou, Y.; Sun, R.; and Li, S. Z. 2024. GeoAB: towards realistic antibody design and reliable affinity maturation. *bioRxiv*, 2024–05.

Luo, S.; Su, Y.; Peng, X.; Wang, S.; Peng, J.; and Ma, J. 2022. Antigen-specific antibody design and optimization with diffusion-based generative models for protein structures. *Advances in Neural Information Processing Systems*, 35: 9754–9767.

Mariani, V.; Biasini, M.; Barbato, A.; and Schwede, T. 2013. lDDT: a local superposition-free score for comparing protein structures and models using distance difference tests. *Bioinformatics*, 29(21): 2722–2728.

Martinkus, K.; Ludwiczak, J.; Liang, W.-C.; Lafrance-Vanasse, J.; Hotzel, I.; Rajpal, A.; Wu, Y.; Cho, K.; Bonneau, R.; Gligorijevic, V.; et al. 2023. Abdiffuser: full-atom generation of in-vitro functioning antibodies. *Advances in Neural Information Processing Systems*, 36: 40729–40759.

Maynard, J.; and Georgiou, G. 2000. Antibody engineering. *Annual review of biomedical engineering*, 2(1): 339–376.

Pantazes, R.; and Maranas, C. D. 2010. OptCDR: a general computational method for the design of antibody complementarity determining regions for targeted epitope binding. *Protein Engineering, Design & Selection*, 23(11): 849–858.

Qi, C. R.; Su, H.; Mo, K.; and Guibas, L. J. 2017. Pointnet: Deep learning on point sets for 3d classification and segmentation. In *Proceedings of the IEEE conference on computer vision and pattern recognition*, 652–660.

Ren, Z.; Li, J.; Ding, F.; Zhou, Y.; Ma, J.; and Peng, J. 2022. Proximal exploration for model-guided protein sequence design. In *International Conference on Machine Learning*, 18520–18536. PMLR.

Ruffolo, J. A.; Chu, L.-S.; Mahajan, S. P.; and Gray, J. J. 2023. Fast, accurate antibody structure prediction from deep learning on massive set of natural antibodies. *Nature communications*, 14(1): 2389.

Saka, K.; Kakuzaki, T.; Metsugi, S.; Kashiwagi, D.; Yoshida, K.; Wada, M.; Tsunoda, H.; and Teramoto, R. 2021. Antibody design using LSTM based deep generative model from phage display library for affinity maturation. *Scientific reports*, 11(1): 5852.

Satorras, V. G.; Hoogeboom, E.; and Welling, M. 2021. E (n) equivariant graph neural networks. In *International conference on machine learning*, 9323–9332. PMLR.

Shan, S.; Luo, S.; Yang, Z.; Hong, J.; Su, Y.; Ding, F.; Fu, L.; Li, C.; Chen, P.; Ma, J.; et al. 2022. Deep learning guided optimization of human antibody against SARS-CoV-2 variants with broad neutralization. *Proceedings of the National Academy of Sciences*, 119(11): e2122954119.

Shin, J.-E.; Riesselman, A. J.; Kollasch, A. W.; McMahon, C.; Simon, E.; Sander, C.; Manglik, A.; Kruse, A. C.; and Marks, D. S. 2021. Protein design and variant prediction using autoregressive generative models. *Nature communications*, 12(1): 2403.

Steinegger, M.; and Söding, J. 2017. MMseqs2 enables sensitive protein sequence searching for the analysis of massive data sets. *Nature biotechnology*, 35(11): 1026–1028.

Taylor, P. C.; Adams, A. C.; Hufford, M. M.; De La Torre, I.; Winthrop, K.; and Gottlieb, R. L. 2021. Neutralizing monoclonal antibodies for treatment of COVID-19. *Nature Reviews Immunology*, 21(6): 382–393.

Warszawski, S.; Borenstein Katz, A.; Lipsh, R.; Khmelnitsky, L.; Ben Nissan, G.; Javitt, G.; Dym, O.; Unger, T.; Knop, O.; Albeck, S.; et al. 2020. Correction: Optimizing antibody affinity and stability by the automated design of the variable light-heavy chain interfaces. *PLoS computational biology*, 16(10): e1008382.

Yan, Y.; Tao, H.; He, J.; and Huang, S.-Y. 2020. The HDOCK server for integrated protein–protein docking. *Nature protocols*, 15(5): 1829–1852.

Yoo, J.-W.; Irvine, D. J.; Discher, D. E.; and Mitragotri, S. 2011. Bio-inspired, bioengineered and biomimetic drug delivery carriers. *Nature reviews Drug discovery*, 10(7): 521–535.

Zhang, Y.; and Skolnick, J. 2004. Scoring function for automated assessment of protein structure template quality. *Proteins: Structure, Function, and Bioinformatics*, 57(4): 702–710.

Zhou, X.; Xue, D.; Chen, R.; Zheng, Z.; Wang, L.; and Gu, Q. 2024. Antigen-specific antibody design via direct energy-based preference optimization. *Advances in Neural Information Processing Systems*, 37: 120861–120891.